Reduced Integration and Differentiation of the Imitation Network in Autism: A Combined Functional Connectivity Magnetic Resonance Imaging and Diffusion-Weighted Imaging Study

Inna Fishman PhD,[1] Michael Datko MS,[2] Yuliana Cabrera BA,[1]
Ruth A. Carper PhD,[1] and Ralph-Axel Müller PhD[1]

Objective: Converging evidence indicates that brain abnormalities in autism spectrum disorder (ASD) involve atypical network connectivity, but few studies have integrated functional with structural connectivity measures. This multimodal investigation examined functional and structural connectivity of the imitation network in children and adolescents with ASD, and its links with clinical symptoms.
Methods: Resting state functional magnetic resonance imaging and diffusion-weighted imaging were performed in 35 participants with ASD and 35 typically developing controls, aged 8 to 17 years, matched for age, gender, intelligence quotient, and head motion.
Results: Within-network analyses revealed overall reduced functional connectivity (FC) between distributed imitation regions in the ASD group. Whole brain analyses showed that underconnectivity in ASD occurred exclusively in regions belonging to the imitation network, whereas overconnectivity was observed between imitation nodes and extraneous regions. Structurally, reduced fractional anisotropy and increased mean diffusivity were found in white matter tracts directly connecting key imitation regions with atypical FC in ASD. These differences in microstructural organization of white matter correlated with weaker FC and greater ASD symptomatology.
Interpretation: Findings demonstrate atypical connectivity of the brain network supporting imitation in ASD, characterized by a highly specific pattern. This pattern of underconnectivity within, but overconnectivity outside the functional network is in contrast with typical development and suggests reduced network integration and differentiation in ASD. Our findings also indicate that atypical connectivity of the imitation network may contribute to ASD clinical symptoms, highlighting the role of this fundamental social cognition ability in the pathophysiology of ASD.

ANN NEUROL 2015;78:958–969

Extensive neuroimaging and electrophysiological evidence accumulated over the past decade indicates that autism spectrum disorder (ASD) is characterized by disrupted neural connectivity and atypical brain network organization.[1–4] Studies utilizing functional connectivity magnetic resonance imaging (fcMRI), which assesses coordination between distributed brain regions, have demonstrated widespread abnormalities in functional connectivity (FC) in ASD.[4] The precise pattern of the FC abnormalities is still unclear, with findings ranging from reduced connectivity (reviewed in Schipul et al.[3]) to partial or even extensive overconnectivity.[5–9] These seemingly contradictory findings may be explained by impaired network differentiation in ASD,[5,6,10] given observations of reduced connectivity within neurotypical networks and diffuse overconnectivity with regions

View this article online at wileyonlinelibrary.com. DOI: 10.1002/ana.24533

Received Apr 21, 2015, and in revised form Sep 9, 2015. Accepted for publication Sep 14, 2015.

Address correspondence to Dr Fishman, Brain Development Imaging Laboratory, Department of Psychology, San Diego State University, 6363 Alvarado Ct, Suite 200, San Diego, CA 92120. E-mail: ifishman@mail.sdsu.edu

From the [1]Department of Psychology, San Diego State University; and [2]Department of Cognitive Science, University of California, San Diego

Additional supporting information can be found in the online version of this article

outside of the networks of interest. This pattern, observed in ASD samples across multiple functional domains and networks,[6,10–12] contrasts with typical development, during which functional brain networks become simultaneously more integrated (within-network connections strengthen) and segregated (between-network connections weaken).[13–15] Additionally, studies utilizing diffusion tensor imaging (DTI) have shown widespread abnormalities of white matter tracts in children and adults with ASD (reviewed in Travers et al.[16]). These aberrant anatomical and functional connections may be at the root of ASD symptomatology (rather than being epiphenomenal), given recent reports of abnormal anatomical[17,18] and functional[19,20] connectivity in infants who later develop ASD.

However, this extensive evidence of atypical brain connectivity has predominantly come from single imaging modality investigations, yielding little insight into the interplay between structural connectivity (SC) and functional network organization. The current study utilizes a multimodal approach, incorporating functional and SC measures in the same cohort of participants, to examine the organization and functioning of the imitation network in children and adolescents with ASD. Deficits in imitation abilities observed in early development in ASD are thought to give rise to a wide range of sociocommunicative impairments associated with ASD.[21,22] Investigations in the field of social psychology demonstrated that imitation is integral to many aspects of social behavior, including emotion recognition, empathy, trust, and rapport.[23–25] Thus, given the primacy of social functioning deficits in individuals with ASD, and the behavioral,[21,26,27] physiological,[28,29] and neuroimaging[30,31] evidence of imitation deficits observed in children and adults with ASD, investigation of imitation network connectivity may be a key to understanding the nature of social dysfunction in ASD.

To this end, we utilized fcMRI and diffusion-weighted imaging (DWI) to examine FC and SC of the imitation network in children and adolescents with ASD. fcMRI assesses whether spatially segregated cortical areas exhibit correlated neural activity, thereby forming coherent functional networks,[32] which are in turn shown to correspond to specific cognitive and mental functions.[33,34] In contrast, DWI assesses SC by quantifying the diffusion of water molecules in neural tissue, and especially in white matter, where water diffusion is hindered by axonal membranes and other cellular structures, resulting in preferential diffusion parallel to fiber bundles. DWI thus allows inferences about the organization and microstructure of white matter tracts, which link cortical areas into functional circuits. Although the importance of white matter fiber pathways in shaping functional brain networks has been generally established,[35,36] functional connections can also exist between 2 regions without direct anatomical connections,[37,38] likely due to polysynaptic connectivity or shared input from a third region. In light of this, we assessed SC only in main tracts directly connecting key nodes of the imitation network, defined according to a recent activation likelihood estimation (ALE) meta-analysis.[39]

The present study investigated whether children and adolescents with ASD show altered functional and SC within a network associated with imitation, a social cognition domain putatively impaired in ASD, by combining resting state fcMRI and DWI. It was hypothesized that individuals with ASD would exhibit altered FC and SC compared to matched typically developing (TD) controls, and that the atypical connectivity patterns would correlate with ASD clinical symptoms. A further aim was to examine whether connectivity patterns within the ASD group changed as a function of age, between ages 8 and 17 years.

Subjects and Methods

Participants

Fifty children and adolescents with ASD and 45 TD participants, aged 8 to 17 years, were enrolled in the study. After excluding 15 ASD and 8 TD participants due to excessive head motion during fMRI (as defined below) and 2 TD participants due to hardware malfunction, the final sample included 35 ASD and 35 TD participants with usable fMRI data matched for age, gender, handedness, nonverbal intelligence quotient (IQ), and head motion (Table 1). Of these, 8 ASD and 7 TD participants were excluded from diffusion analyses due to excessive motion or other imaging artifacts during diffusion scans (as detailed below), leaving 27 ASD and 28 TD participants for the combined FC-DWI analyses (Table 2). The ASD and TD groups in both the full sample and the subset with usable data in both modalities (henceforth, the FC-DWI subset) did not significantly differ on age, IQ, or motion (FC- or DWI-specific) parameters. ASD diagnoses were made based on Diagnostic and Statistical Manual of Mental Disorders IV-TR criteria[40] and were supported by the Autism Diagnostic Interview, Revised[41] and the Autism Diagnostic Observation Schedule (ADOS).[42] Participants with history of autism-related medical (eg, epilepsy, tuberous sclerosis) or genetic conditions (eg, fragile X, Rett syndrome) were excluded. Inclusion in the TD group required absence of personal or family history of autism, and of personal history of any other neurological or psychiatric conditions. Participants with ASD with comorbid attention-deficit/hyperactivity disorder, obsessive–compulsive disorder, or anxiety disorders were not excluded, because of the high prevalence of such conditions in children and adolescents with ASD.[43] IQ was assessed by the Wechsler Abbreviated Scale of Intelligence, 2nd edition.[44] In addition to the ADOS-derived indices of social behavior available only for ASD participants,

TABLE 1. Participant Characteristics in the Full Sample Used for FC Analyses

Characteristic	ASD, n = 35	TD, n = 35	TD vs ASD, *p*
Gender, M/F[a]	31/4	28/7	0.14
Handedness, R/L[a]	30/5	30/5	0.96
Age, yr, mean ± SD (range)	13.7 ± 2.4 (9.2–17.7)	13.2 ± 2.5 (8.7–17.6)	0.40
Verbal IQ, mean ± SD (range)	106 ± 19 (70–147)	109 ± 10 (87–133)	0.40
Nonverbal IQ, mean ± SD (range)	107 ± 17 (53–140)	107 ± 11 (86–129)	0.99
Full-scale IQ, mean ± SD (range)	107 ± 18 (66–141)	109 ± 10 (88–132)	0.58
ADOS, mean ± SD (range)			
Communication	4.0 ± 2.4 (1–13)	n/a	—
Social interaction	8.2 ± 2.8 (3–14)	n/a	—
Repetitive behavior	2.1 ± 1.4 (1–4)	n/a	—
ADI-R, mean ± SD (range)			
Social interaction	18.4 ± 5.8 (6–28)	n/a	—
Communication	14.1 ± 5.9 (2–24)	n/a	—
Repetitive behavior	6.3 ± 2.2 (3–11)	n/a	—
SRS, total, mean ± SD (range)	81 ± 9 (58–94)	42 ± 5 (35–52)	0.000
RMSD, FC head motion, mean ± SD (range)	0.066 ± 0.04 (0.02–0.15)	0.063 ± 0.03 (0.02–0.15)	0.71

Thirteen ASD participants presented with comorbid psychiatric conditions, including attention-deficit/hyperactivity disorder (n = 6), obsessive–compulsive disorder (n = 1), depression (n = 6), and anxiety (n = 7); 2 of 13 were diagnosed with > 1 comorbid condition. Eleven ASD participants were reported to be on psychoactive medications.
[a]Values denote counts and corresponding chi-square *p* values.
ADI-R = Autism Diagnostic Interview, Revised; ADOS = Autism Diagnostic Observation Schedule; ASD = autism spectrum disorder; F = female; FC = functional connectivity; IQ = intelligence quotient; L = left; M = male; n/a = not applicable; R = right; RMSD = root mean square of displacement; SD = standard deviation; SRS = Social Responsiveness Scale; TD = typically developing.

social functioning was also assessed in all participants using the Social Responsiveness Scale (SRS).[45] Hand preference was assessed with the Edinburgh handedness inventory.[46] Informed assent and consent were obtained from all participants and their caregivers in accordance with the University of California, San Diego and San Diego State University institutional review boards.

MRI Data Acquisition

Imaging data were acquired on a GE (Milwaukee, WI) 3T MR750 scanner with an 8-channel head coil. High-resolution anatomical images were obtained using a standard T1-weighted inversion recovery spoiled gradient echo sequence (repetition time [TR] = 8.108 milliseconds, echo time [TE] = 3.172 milliseconds, flip angle = 8°, 172 slices, $1mm^3$ resolution). Functional T2*-weighted images were acquired using a single-shot gradient-recalled, echo-planar pulse sequence, in one 6:10-minute resting state scan consisting of 185 whole brain volumes (TR = 2,000 milliseconds, TE = 30 milliseconds, flip angle = 90°, field of view [FOV] = 220mm, 64×64 matrix, $3.4 \times 3.4 \times 3.4mm^3$ resolution, 42 axial slices covering the whole brain). Throughout the resting state scan, participants were instructed to relax, and to keep their eyes open and centered on a white fixation cross displayed on black background in the center of a screen, using a rear projection display. Diffusion-weighted images were obtained with an echo-planar pulse sequence with full head coverage and encoded for 61 noncollinear diffusion directions at $b = 1{,}000s/mm^2$, and 1 at $b = 0s/mm^2$, with a dual spin echo excitation to reduce eddy current artifacts (TR = 8,500 milliseconds, TE = 84.9 milliseconds, flip angle = 90°, FOV = 240mm, 128×128 matrix, $1.88 \times 1.88 \times 2mm^3$ resolution). Total diffusion-weighted scan time was about 9 minutes. Field maps were collected for fMRI and DWI scans with the same spatial parameters to correct for field inhomogeneities (TR = 1,097 milliseconds, TE = 9.5 milliseconds, flip angle = 45°, 2 averages).

fMRI Data Preprocessing and fcMRI Analyses

Images were processed using Analysis of Functional NeuroImages[47] and FMRIB Software Library (FSL).[48] After discarding

TABLE 2. Participant Characteristics in the FC-DWI Subset

Characteristic	ASD, n = 27	TD, n = 28	TD vs ASD, *p*
Gender, M/F[a]	24/3	21/7	0.12
Handedness, R/L[a]	25/5	25/4	0.63
Age, yr, mean ± SD (range)	13.7 ± 2.3 (9.6–17.7)	13.4 ± 2.4 (8.7–17.6)	0.66
Verbal IQ, mean ± SD (range)	105 ± 21 (70–147)	107 ± 10 (87–127)	0.60
Nonverbal IQ, mean ± SD (range)	108 ± 16 (53–140)	107 ± 11 (86–129)	0.78
Full-scale IQ, mean ± SD (range)	106 ± 19 (66–141)	108 ± 10 (88–126)	0.75
ADOS, mean ± SD (range)			
Communication	3.7 ± 1.9 (1–8)	n/a	—
Social interaction	8.7 ± 2.7 (5–14)	n/a	—
Repetitive behavior	2.0 ± 1.4 (1–4)	n/a	—
ADI-R, mean ± SD (range)			
Social interaction	17.2 ± 6.0 (6–28)	n/a	—
Communication	12.8 ± 6.1 (2–24)	n/a	—
Repetitive behavior	6.2 ± 2.4 (3–11)	n/a	—
SRS, total, mean ± SD (range)	82 ± 8 (64–94)	42 ± 5 (35–52)	0.000
RMSD, FC head motion, mean ± SD (range)	0.066 ± 0.04 (0.02–0.15)	0.058 ± 0.03 (0.02–0.15)	0.41
DMI, DWI head motion, mean ± SD (range)	0.92 ± 0.42 (0.0–2.35)	0.97 ± 0.29 (0.59–1.74)	0.62

[a]Values denote counts and corresponding chi-square *p* values.
ADI-R = Autism Diagnostic Interview, Revised; ADOS = Autism Diagnostic Observation Schedule; ASD = autism spectrum disorder; DMI = diffusion motion index; DWI = diffusion-weighted imaging; F = female; FC = functional connectivity; IQ = intelligence quotient; L = left; M = male; n/a = not applicable; R = right; RMSD = root mean square of displacement; SD = standard deviation; SRS = Social Responsiveness Scale; TD = typically developing.

the first 5 volumes to remove signal equilibration effects, data were slice-time and motion corrected by realigning to the middle time point, field-map corrected to remove distortions resulting from magnetic field inhomogeneity, coregistered to the anatomical image using FSL's FLIRT, resampled to 3.0mm isotropic voxels, and standardized to the Montreal Neurological Institute (MNI) template with FSL's FNIRT. The resulting images were band-pass filtered at $0.008 < f < 0.08$Hz, using a second-order Butterworth filter, to isolate frequencies at which intrinsic network-specific blood oxygenation level–dependent (BOLD) correlations predominate,[49,50] and spatially smoothed to a global full width at half maximum of 6mm. Six motion parameters, mean white matter and ventricular (cerebrospinal fluid [CSF]) signals (extracted from participant-level masks created with FSL's FAST automated segmentation and eroded to avoid partial-volume effects), and their first temporal derivatives (all band-pass filtered at $0.008 < f < 0.08$Hz) were regressed from the signal.

To minimize the known impact of motion on fcMRI effects,[51,52] time points with > 0.5mm head motion in any direction and 2 subsequent time points were censored from further analyses, and blocks of time points with <10 usable consecutive images were also excluded. Based on these criteria, 15 of 50 participants with ASD and 8 of 45 TD participants were excluded from further analyses. The mean percentage of censored time points in the final sample of 35 ASD and 35 TD participants did not differ between groups ($M_{ASD} = 1.8\%$, $M_{TD} = 1.3\%$, $p = 0.62$), nor did the individual motion parameters (translation and rotation for each brain volume in the x, y, and z planes; all *p*s = 0.43–0.93) or the mean head motion (computed as the root mean square of displacement [RMSD] on all 6 translational and rotational axes; see Table 1).

Seeds were placed in 14 regions of interest (ROIs) found to be consistently activated by imitation tasks, as determined by a ALE meta-analysis[39] based on 139 fMRI imitation experiments. The seeds included regions in the bilateral inferior frontal gyri (IFG), lateral–dorsal premotor cortex (PMC), medial PMC, lateral occipital cortices (LOCs, corresponding to area V5), primary somatosensory cortex/inferior parietal lobule (IPL), right anterior insula, right fusiform cortex (fusiform face

area [FFA] and fusiform body area), right secondary somatosensory cortex (parietal operculum), and left superior temporal sulcus (STS; see Fig 1A for seed placements and MNI coordinates). Seeds were created using 6mm-radius spheres around peak coordinates (discarding voxels with > 20% nongray partial volume), covering between 29 and 33 voxels in $3mm^3$ space. Average BOLD time series extracted from each seed were correlated with the time courses of all voxels across the brain, for every participant. The resulting voxelwise correlation coefficients were converted to normally distributed z values (using Fisher r-to-z transformation) and entered into 1 and 2 independent sample t tests to examine within- and between-group FC effects, utilizing Monte Carlo simulation to correct for multiple comparisons.

DWI Data Preprocessing, Selection of Tracts, and Tractography

Images were processed using FSL.[48] After applying field-map correction of magnetic field inhomogeneity, resampling to 1.0mm isotropic voxels, and correcting for eddy current distortions, all data including each diffusion direction in all 3 planes of view were visually inspected and rated for motion-related artifacts, to minimize the effects of head motion on diffusion measures.[53,54] Images were rated for shifts of head placement

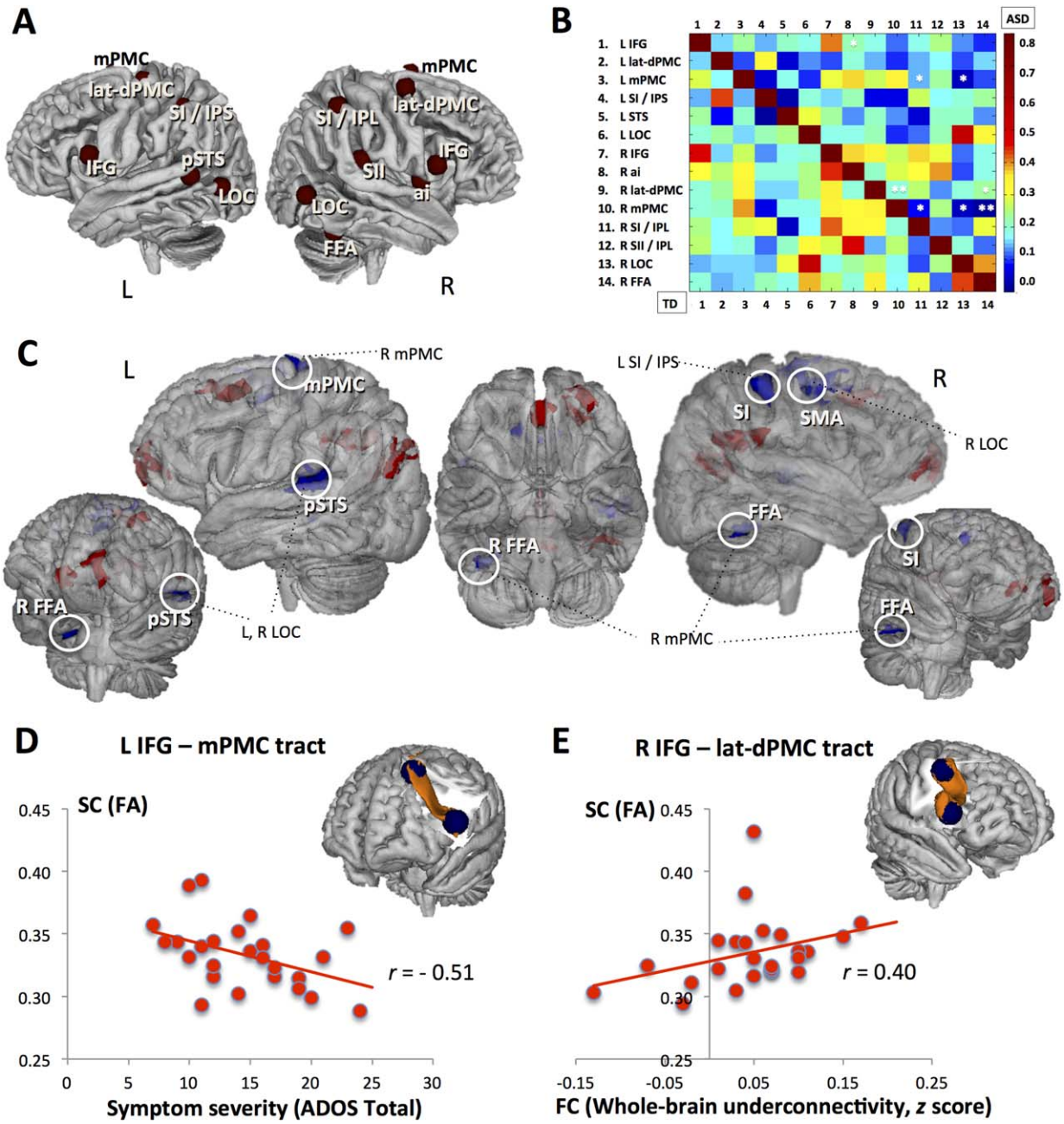

FIGURE :1.

between acquisition of individual diffusion directions, signal dropout, and image noise. Scans with evidence of moderate to severe motion[54] were excluded from analyses. A diffusion motion index (DMI) was calculated based on the mean image translation and rotation applied during eddy correction and the frequency of signal dropouts across all slices (modified from Yendiki et al.[54]). The ASD and TD groups were matched on all individual motion and signal dropout indices (all $ps = 0.59$–0.71) and the DMI (see Table 2); the DMI was also used as a covariate in all diffusion analyses.[54] FSL's Diffusion Toolbox was used to calculate the diffusion tensors at each voxel and derive mean diffusivity (MD) and fractional anisotropy (FA), summative measures that describe average water diffusion within a given voxel and directionality of water diffusion on a scale from 0 (random diffusion) to 1 (unidirectional diffusion). The FA maps were registered nonlinearly to the FMRIB58 FA template in MNI standard space, and resulting transformation matrices were used in conversion between standard (seed) and native space.

Fiber tracking was performed in native space using FSL's BEDPOSTX and ProbtrackX.[48,53] Tractography seeds were spheres defined by the same coordinates used for fcMRI analyses. To ensure inclusion of underlying white matter voxels, larger spheres (10mm radius) were used and seeds were nudged toward the local gray–white matter boundary, until at least 40% of voxels within each seed had $FA > 0.2$ (mean = 54% of voxels, range = 40–74%). These steps were necessary to increase projection from the functionally defined gray matter ROIs into adjacent white matter[55] (see Supplementary Methods and Supplementary Fig for more details). Rather than examine all possible tracts linking 91 ROI pairs—many of which would be anatomically implausible—tractography was limited to a subset of tracts that (1) were consistent with known white matter pathways, (2) were connected imitation regions showing significant group effects in FC (Supplementary Table 1), and (3) were reliably identifiable with DWI in our sample. Of these, only intrahemispheric connections were considered, to avoid major areas of crossing fibers within the centrum semiovale.[56,57] Anatomical validity of the resulting tracts was established using white matter atlases[58] and published literature.[59] Tracts were considered reliable if at least 93% of participants (ie, all but 2 individuals) from each group had at least 0.01% of the initiated streamlines reaching the target ROI (see Supplementary Table 2 for tract identification rates and final set of tracts of interest [TOIs]).

For each TOI, 1,000 streamlines were initiated per seed voxel (ie, from ROI1 to ROI2, and from ROI2 to ROI1), propagating with 0.5mm step length and curvature threshold of 0.2. Streamlines reaching the other ROI were selected, resulting in a probability map of tract location effectively based on 2,000 initiated streamlines per ROI pair. A minimum threshold of 150 streamlines was applied to form a binary mask of each subject-specific TOI. Mean FA and MD values were calculated for each TOI using these masks; tract volumes were calculated as a measure of overall size of the thresholded TOIs in native space. Finally, total brain volume (TBV) including all brain parenchyma but excluding CSF was derived from the eddy-corrected diffusion data using the b = 0 images.

Results

FC

Whole brain within-group FC analyses performed for each of the imitation seeds revealed largely overlapping FC clusters spanning the key imitation regions,[39] including bilateral IFG, dorsolateral and medial PMCs, IPL,

FIGURE 1: (A) Imitation network seeds. ai = anterior insula (Montreal Neurological Institute [MNI] coordinates = 42, 4, 1); FFA = fusiform area (44, −54, −22); IFG = inferior frontal gyrus (−60, 12, 14 and 58, 16, 10, left and right, respectively); SI/IPL = primary somatosensory cortex/inferior parietal lobule (52, −36, 52); L = left; lat-dPMC = lateral dorsal premotor cortex (−36, −14, 62 and 42, 4, 56); LOC = lateral occipital cortex/area V5 (−52, −70, 6 and 54, −64, 4); mPMC = medial premotor cortex (−1, 12, 52 and 14, 6, 66); SI/IPS = primary somatosensory cortex/intraparietal sulcus (−38, −40, 50); pSTS = posterior superior temporal sulcus; R = right; SII/IPL = secondary somatosensory cortex/inferior parietal lobule (60, −26, 20); STS = superior temporal sulcus (−54, −50, 10). (B) Imitation network cross-correlation matrix. Normalized pairwise correlation coefficients are reported separately for the autism spectrum disorder (ASD; upper triangle) and typically developing (TD; lower triangle) groups. Both axes represent the 14 imitation seed regions; pixel color of each cell represents the magnitude of correlation for each region of interest (ROI) pair, with warmer colors indicating greater correlation coefficient values. Asterisks indicate ROI pairs with significantly weaker connections in the ASD group (* and ** indicate uncorrected $p < 0.05$ and $p < 0.01$, respectively). (C) Between-group differences (ASD vs TD) in functional connectivity (FC) of the imitation network. Clusters of significantly different FC ($p < 0.01$ corrected) in ASD participants relative to the TD group are presented in a conjunction view (overlaid on the FMRIB Software Library 3DView standard brain). Statistical maps for those seeds yielding significant clusters (described in Table 2) were combined separately for under- and overconnected clusters (indicated with blue and red colors, respectively). White circles mark (exclusively underconnected) clusters that overlap with the imitation seed regions (see also A), with corresponding seed ROIs. The unmarked (overconnected) clusters all fall outside of the imitation network. SMA = supplementary motor area. (D) Relationship between structural connectivity (SC) and ASD symptom severity. Three-dimensional (3D) representation shows the tract connecting left IFG and left medial PMC (results for the ASD group are shown over a standard MNI reference image after thresholding the probability map; the 2 blue spheres represent seed regions used for tractography). The scatterplot below shows the relationship between fractional anisotropy (FA) of this tract and ASD symptom severity, as measured with the Autism Diagnostic Observation Schedule (ADOS) total score ($r[27] = -0.51$, $p = 0.01$). Increasing ADOS total values indicate greater symptom count and hence greater impairment. (E) Cross-modal relationship between SC and FC. 3D representation shows the tract connecting right IFG and right lateral dorsal PMC (results for the ASD group are shown over a standard MNI reference image after thresholding the probability map; the 2 blue spheres represent seed regions used for tractography). The scatterplot below shows the relationship between FA of this tract and the whole brain functional underconnectivity of the imitation network, expressed as an average *z* score for all underconnected clusters ($r[27] = 0.40$, $p = 0.045$).

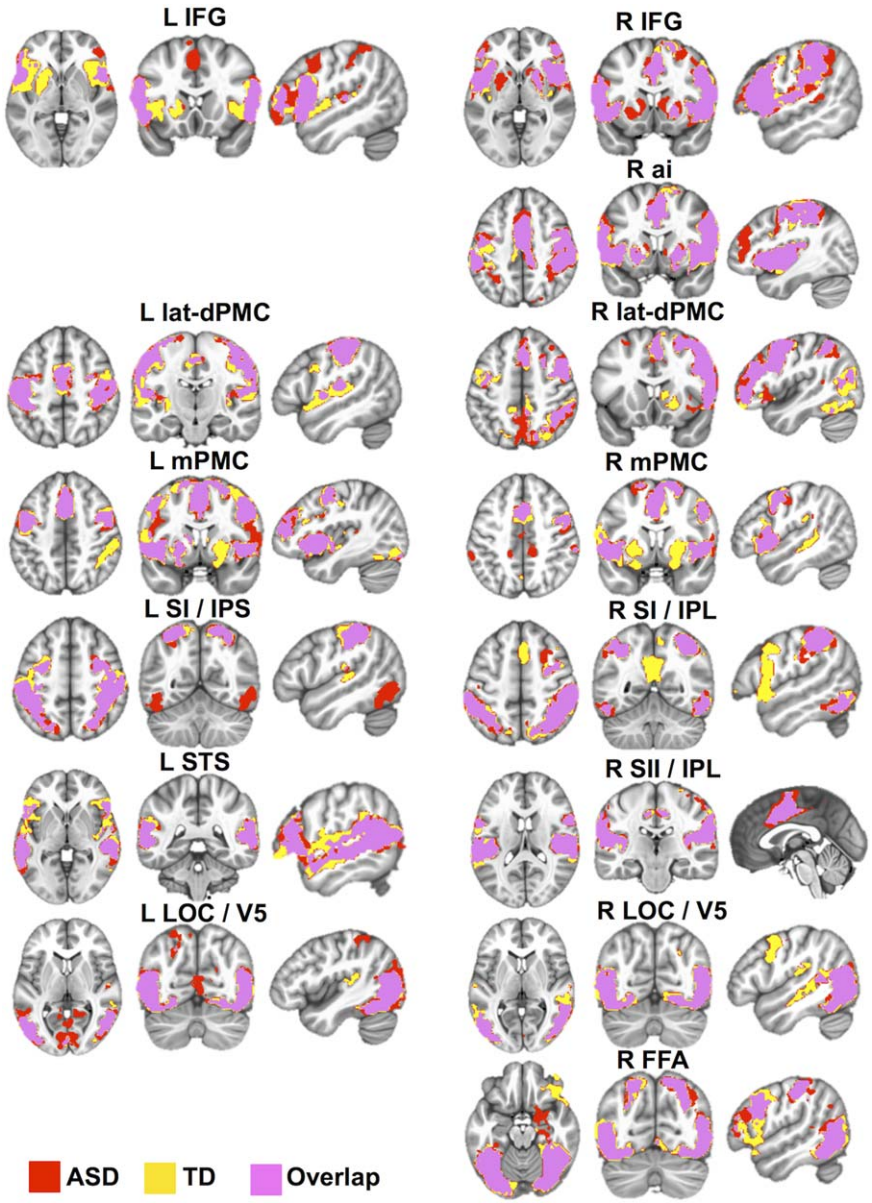

FIGURE 2: Within-group functional connectivity maps for the key imitation seed regions. Results of the within-group (autism spectrum disorder [ASD], typically developing [TD]; $p<10^{-4}$ corrected) analyses for each imitation seed are presented in a conjunction view. Yellow and red areas denote clusters of significant functional connectivity for the TD and ASD groups, respectively, with pink regions demonstrating their overlap. L IFG = left inferior frontal gyrus (seed Montreal Neurological Institute coordinates = −60, 12, 14); R IFG = right inferior frontal gyrus (58, 16, 10); R ai = right anterior insula (42, 4, 1); L lat-dPMC = left lateral dorsal premotor cortex (−36, −14, 62); R lat-dPMC = right lateral dorsal premotor cortex (42, 4, 56); L mPMC = left medial premotor cortex (−1, 12, 52); R mPMC = right medial premotor cortex (14, 6, 66); L SI/IPS = left primary somatosensory cortex/intraparietal sulcus (−38, −40, 50); R SI/IPL = right primary somatosensory cortex/inferior parietal lobule (52, −36, 52); L STS = left superior temporal sulcus (−54, −50, 10); R SII/IPL = right secondary somatosensory cortex/inferior parietal lobule (60, −26, 20); L LOC/V5 = left lateral occipital cortex/area V5 (−52, −70, 6); R LOC/V5 = right lateral occipital cortex/area V5 (54, −64, 4); R FFA = right fusiform area (44, −54, −22).

LOCs, and fusiform gyrus (Fig 2; see also Supplementary Table 3 for detailed descriptions, including peak coordinates). Whereas some seeds (eg, left lateral dorsal PMC, left STS) yielded quite similar clusters in both groups, other seed regions had more dissimilar FC patterns between the groups. For instance, in the ASD group, right LOC showed connectivity with itself and its contralateral homologue, whereas in the TD group this seed was also significantly connected with other imitation regions, such as medial and bilateral PMC/supplementary motor area (SMA) and ipsilateral IPL. Moreover, for some seeds, significant connectivity was detected with regions outside the

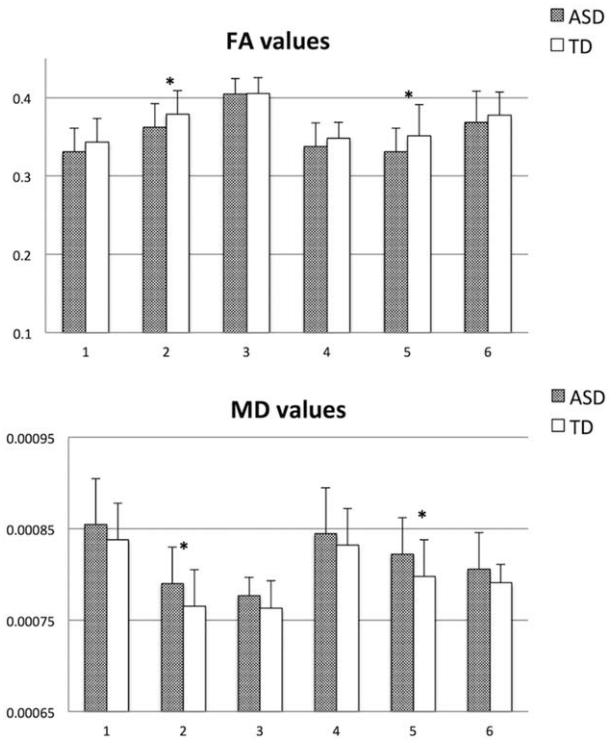

FIGURE 3: Fractional anisotropy (FA) and mean diffusivity (MD) means in white matter tracts of interest in autism spectrum disorder (ASD) and typically developing (TD) groups. 1 = Left inferior frontal gyri (IFG) to left medial premotor cortex (PMC); 2 = left IFG to left lateral dorsal PMC; 3 = left IFG to left intraparietal sulcus; 4 = right IFG to right medial PMC; 5 = right IFG to right lateral dorsal PMC; 6 = right IFG to right inferior parietal lobule. *Statistical significance with $p < 0.05$.

imitation network, to a different extent in the 2 groups. For instance, in addition to significant FC clusters in bilateral IFG, left IFG had significant connectivity with left thalamus in the TD but not in the ASD group; right IFG, right medial PMC, and right IPL all showed significant connectivity with precuneus in TD but not in ASD children (see Fig 2; see Supplementary Table 3).

Direct group comparisons (corrected $p < 0.01$) revealed several significant clusters of differential connectivity for 7 of the 14 seeds, with clusters of both increased (ASD > TD) and decreased (ASD < TD) connectivity (see Fig 1C and Supplementary Table 1). Overall, left IFG and right lateral dorsal PMC yielded clusters of exclusively greater connectivity in ASD, whereas left IPL, right medial PMC, and the bilateral LOCs all yielded exclusively underconnected clusters (ASD < TD). The right FFA exhibited mixed connectivity effects, with both overconnected (ASD > TD) and underconnected (ASD < TD) clusters. As highlighted in Figure 1C, a closer examination of the between-group differences and their regional specificity (see Supplementary Table 1) revealed that clusters with weaker connectivity in the ASD group almost exclusively encompassed regions belonging to the imitation network (eg, left primary somatosensory cortex [SI]/intraparietal sulcus [IPS] was underconnected with the right SI; bilateral LOCs were underconnected with left posterior STS; right medial PMC, right LOC, and right FFA were all underconnected with right medial SMA/PMC). Conversely, all clusters of significant ASD-related overconnectivity contained regions extraneous to the imitation network (eg, precuneus and posterior cingulate, angular gyrus, frontal eye fields, superior orbital gyrus, and frontopolar prefrontal cortex).

A 14×14 connectivity matrix of all imitation ROI pairs, calculated separately for each group, revealed overall lower within-network correlations in participants with ASD, with more links with close to zero correlation values (represented by deep blue color in Fig 1B) in the ASD group. Direct group comparison (uncorrected $p < 0.05$) showed significantly lower correlations (ASD < TD) between several, mostly right seed regions, including right lateral dorsal PMC with both right medial PMC and right FFA; and right medial PMC with right IPL, LOC, and FFA (see Fig 1B).

Structural Connectivity

Two repeated measures analyses of covariance (ANCOVAs), conducted separately for FA and MD, with TOI as a within-subjects repeated variable, group as a between-subjects variable, and DMI and age as covariates, revealed significant group effects. Namely, adjusted for DMI and age, the ASD group had lower FA ($F_{1,53} = 5.4$, $p = 0.03$, partial $\eta^2 = 0.11$) and higher MD values ($F_{1,53} = 5.8$, $p = 0.02$, partial $\eta^2 = .11$) across all TOIs (Fig 3). Follow-up pairwise comparisons (univariate analyses of variance, with DMI and age as covariates) revealed that these group effects were particularly driven by the tracts connecting IFG and lateral dorsal PMC, bilaterally (left: $p_{FA} = 0.045$, $p_{MD} = 0.015$; right: $p_{FA} = 0.046$, $p_{MD} = 0.045$; see Fig 3). There were neither significant group × TOI interaction effects nor significant relationships with the DMI covariate ($ps > 0.80$). Age was a significant covariate for FA ($p = 0.03$), but not for MD ($p = 0.27$). Repeated measures ANCOVA performed for tract volumes, with age, DMI, and TBV as covariates (the latter included to control for individual differences in overall brain size), revealed no significant effects.

Age Effects on FC and SC

Relationships between age and FC scores were examined with partial correlations, controlling for RMSD. To minimize multiple comparisons, 3 FC summary measures were calculated: the overall imitation network FC (NetFC), computed by averaging z scores for all

imitation ROI pairs, and atypical under- and overconnectivity in ASD, summarized by separately averaging z scores from all significantly underconnected (ASD < TD) and overconnected (ASD > TD) clusters (henceforth, UnderFC and OverFC, respectively). Whereas no significant correlations were detected between age and FC in the ASD group (all ps = 0.17–0.90), age was significantly correlated with NetFC ($r = 0.37$, $p = 0.03$) and UnderFC ($r = 0.41$, $p = 0.01$) in the TD group. Correlations between age and diffusion parameters in all TOIs were also examined with partial correlations, controlling for DMI. Within the ASD group, age was positively correlated ($r = 0.52$, $p = 0.01$) with FA and negatively correlated ($r = -0.52$, $p = 0.01$) with MD of the tract connecting left IFG to left lateral dorsal PMC, whereas no significant correlations with age were detected within the TD group (all ps > 0.10).

Cross-Modality Correlations and Links with Clinical Measures

Within the ASD group, the relationships between FC and SC of the imitation network and clinical ASD symptoms were examined with partial correlations, controlling for RMSD and DMI. To minimize multiple comparisons (and associated type 1 error), correlational analyses were limited to 1 diagnostic score (the ADOS total score) and 1 sociability score (SRS total); 3 FC summary measures (NetFC, UnderFC, and OverFC); and 6 FA values for TOIs (given the comparable FA and MD effects detected in the above analyses). ADOS total score was negatively correlated with FA of the tract connecting left IFG and left medial PMC ($r = -0.51$, $p = 0.01$), such that lower FA was associated with greater symptom count (see Fig 1D). Cross-modally, significant correlation ($r = 0.40$, $p = 0.045$) was detected between FA of the tract connecting right IFG and right lateral dorsal PMC and UnderFC; that is, lower FA in this tract was associated with reduced FC in clusters of regions belonging to the imitation network (see Fig 1C, E). Finally, a post hoc measure of network sculpting (NetS) was calculated as an UnderFC/OverFC ratio reflecting the relationship between within- and out-of-network FC. There was a significant correlation between ADOS total and NetS ($r = 0.36$, $p = 0.048$).

Discussion

We used resting state fcMRI to examine intrinsic FC of the brain network supporting imitation, and DWI to assess the underlying white matter microstructure of the known pathways connecting key imitation regions, in a sample of 8- to 17-year-old children and adolescents with ASD and matched TD controls. Within-network FC analyses revealed overall reduced brain connectivity between distributed imitation regions in the ASD group. However, whole brain FC analyses showed that underconnectivity in ASD occurred exclusively in regions belonging to the imitation network, whereas many regions outside the neurotypical imitation network were overconnected with imitation nodes. DWI showed aberrant SC in tracts directly connecting key imitation regions that exhibited atypical FC in the ASD group. Specifically, reduced FA and elevated MD were found in tracts connecting IFG and lateral dorsal PMC, bilaterally.

First, the pattern of reduced correlations observed within the imitation network—detected through both within-network and whole brain analyses—is consistent with previous findings in other networks[5,10,60] and indicative of weaker integration of the imitation network in ASD. Conversely, the observation of atypically increased FC detected between imitation nodes and regions belonging to other functional networks (including precuneus and posterior cingulate, angular gyrus, frontal eye fields, superior orbital gyrus, and frontopolar prefrontal cortex) suggests that the imitation network is less functionally segregated from other brain networks in children and adolescents with ASD. This pattern of underconnectivity within, but overconnectivity outside functional networks is in contrast to typical development, during which neural networks become simultaneously more integrated (ie, within-network connections strengthen) and segregated (ie, out-of-network connections weaken).[13–15,60] The observed results, reflecting disruption of such typical pattern, are consistent with our recent findings[5,6] and reports by others[10] supporting reduced network sculpting in ASD. This pattern reflects aberrant network maturation, whereby atypically excessive connections with extraneous regions strengthen secondary to inefficiency of the primary neural circuits. The between-group effects observed here demonstrate this duality of weaker connectivity within, and excessive connectivity outside the brain network supporting imitation—a core component of human social behavior and social understanding, and a domain putatively impaired in ASD.[26–31] This dual impairment was captured by the imitation network sculpting metric (NetS), which was associated with ASD symptomatology, providing further evidence that atypical brain network integration and differentiation may be a core neural feature of ASD.

Second, with respect to SC, significantly reduced FA and increased MD in 2 tracts linking key imitation regions with atypical FC suggest impaired microstructural organization of white matter that integrates this distributed circuit. The tracts connecting IFG and lateral dorsal PMC, bilaterally, are likely part of the superior longitudinal fasciculus (SLF),[58] a major white matter association tract in the human brain, connecting the parietal,

occipital, and temporal lobes with ipsilateral frontal cortices. According to a recent meta-analysis of DTI studies in ASD,[61] the SLF is one of only few consistent sites of reduced anisotropy in ASD (although a recent study[53] in a younger ASD sample with lower symptom severity relative to the current cohort found no such effect). Although underlying cellular properties are not fully understood,[62] the reduced FA and increased MD observed here probably reflect white matter compromise along the tracts linking key imitation regions with atypical FC. Moreover, the observed links between lower anisotropy and weaker functional connections between imitation regions in ASD (UnderFC), as well greater ASD symptomatology, indicate that these white matter abnormalities are related to aberrant FC and ASD core clinical symptoms.

The observed effects of age on connectivity were partly unexpected; whereas no significant age effects on FC were detected in the ASD group, age was positively correlated with within-network FC (NetFC) in TD participants. This suggests that, in TD, the imitation network continues to integrate, or to strengthen its internal connectivity well into adolescence, consistent with the network maturation account.[13–15] This trajectory of increasing network integration with age was entirely absent in our ASD sample. Given the central role that imitation plays in social functioning—providing foundations for understanding actions, behaviors, and by extension intentions of others—this lack of continuing maturation of the neural circuit supporting this fundamental social ability is particularly salient and might contribute to the pervasive nature of sociocommunicative impairment in ASD.

Among limitations of the present study are (1) exclusion of low-functioning children with ASD (due to the extreme sensitivity of fcMRI and to a lesser degree DWI to head motion[51,54]), implying that findings may not generalize to the lower end of the autistic spectrum; (2) use of cross-sectional data to test for age-related effects; (3) use of a common tensor model for tractography with known limitations in resolving complex fiber architectures, which may have prevented identification of tracts in some functionally critical regions (eg, FFA and LOC) and detection of white matter abnormalities in such tracts; and (4) lack of pubertal development measures. Although there is little research in humans on the impact of puberty and associated hormonal changes on maturation of specific brain networks or white matter pathways,[63] there is some evidence pointing to direct links between pubertal maturation and increases in white matter volume in TD males.[64] It is possible that, with a targeted assessment of pubertal hormonal levels, more refined (eg, nonlinear) developmental trajectories of the imitation network connections may have been detected within each group.

In sum, the current results demonstrate atypical functional and SC of the network of regions supporting imitation in a sample of children and adolescents with ASD. Specifically, weaker within-network connections and excessive out-of-network FC, as well as lower FA and higher MD in tracts directly connecting key imitation regions that show atypical FC were detected. These differences in microstructural organization of white matter correlated with weaker FC and greater symptomatology, suggesting that abnormal functional and structural connections between distributed regions involved in imitation contribute to the severity of ASD and persist at least through late adolescence.

Acknowledgment

This work was supported by grants from the NIH National Institute of Mental Health (R01 MH081023, R.A.M.; K01 MH097972, I.F.) and Autism Science Foundation (12-1001, I.F.). Data acquisition in 12 participants was funded by a Congressionally Directed Medical Research Programs grant (AR093335).

We thank the children and families who so generously dedicated their time and effort to this research.

Authorship

Study design and conception: I.F., R.A.C., R.-A.M.; data acquisition and analysis: M.D., Y.C., I.F., R.A.C.; writing manuscript and drafting figures: I.F., M.D., R.A.C.

Potential Conflicts of Interest

Nothing to report.

References

1. Belmonte MK, Cook EH Jr, Anderson GM, et al. Autism as a disorder of neural information processing: directions for research and targets for therapy. Mol Psychiatry 2004;9:646–663.
2. Müller RA. The study of autism as a distributed disorder. Ment Retard Dev Disabil Res Rev 2007;13:85–95.
3. Schipul SE, Keller TA, Just MA. Inter-regional brain communication and its disturbance in autism. Front Syst Neurosci 2011;5:10.
4. Vissers ME, Cohen MX, Geurts HM. Brain connectivity and high functioning autism: a promising path of research that needs refined models, methodological convergence, and stronger behavioral links. Neurosci Biobehav Rev 2012;36:604–625.
5. Shih P, Keehn B, Oram JK, et al. Functional differentiation of posterior superior temporal sulcus in autism: a functional connectivity MRI study. Biol Psychiatry 2011;70:270–277.
6. Fishman I, Keown C, Lincoln AJ, et al. Atypical cross-talk between mentalizing and mirror neuron networks in autism spectrum disorder. JAMA Psychiatry 2014;71:751–760.

7. Supekar K, Uddin LQ, Khouzam A, et al. Brain hyperconnectivity in children with autism and its links with social deficits. Cell Reports 2013;5:738–747.
8. Redcay E, Moran JM, Mavros PL, et al. Intrinsic functional network organization in high-functioning adolescents with autism spectrum disorder. Front Hum Neurosci 2013;7:573.
9. Di Martino A, Kelly C, Grzadzinski R, et al. Aberrant striatal functional connectivity in children with autism. Biol Psychiatry 2011;69: 847–856.
10. Rudie JD, Shehzad Z, Hernandez LM, et al. Reduced functional integration and segregation of distributed neural systems underlying social and emotional information processing in autism spectrum disorders. Cereb Cortex 2012;22:1025–1037.
11. Geschwind DH, Levitt P. Autism spectrum disorders: developmental disconnection syndromes. Curr Opin Neurobiol 2007;17:103–111.
12. Nebel MB, Joel SE, Muschelli J, et al. Disruption of functional organization within the primary motor cortex in children with autism. Hum Brain Mapp 2014;35:567–580.
13. Dosenbach NU, Nardos B, Cohen AL, et al. Prediction of individual brain maturity using fMRI. Science 2010;329:1358–1361.
14. Supekar K, Musen M, Menon V. Development of large-scale functional brain networks in children. PLoS Biol 2009;7:e1000157.
15. Fair DA, Cohen AL, Powers JL, et al. Functional brain networks develop from a "local to distributed" organization. PLoS Comput Biol 2009;5:e1000381.
16. Travers BG, Adluru N, Ennis C, et al. Diffusion tensor imaging in autism spectrum disorder: a review. Autism Res 2012;5:289–313.
17. Weinstein M, Ben-Sira L, Levy Y, et al. Abnormal white matter integrity in young children with autism. Hum Brain Mapp 2011;32:534–543.
18. Wolff JJ, Gu H, Gerig G, et al. Differences in white matter fiber tract development present from 6 to 24 months in infants with autism. Am J Psychiatry 2012;169:589–600.
19. Dinstein I, Pierce K, Eyler L, et al. Disrupted neural synchronization in toddlers with autism. Neuron 2011;70:1218–1225.
20. Keehn B, Wagner JB, Tager-Flusberg H, Nelson CA. Functional connectivity in the first year of life in infants at-risk for autism: a preliminary near-infrared spectroscopy study. Front Hum Neurosci 2013;7:444.
21. Williams JHG, Whiten A, Singh T. A systematic review of action imitation in autistic spectrum disorder. J Autism Dev Disord 2004; 34:285–299.
22. Williams JH, Whiten A, Suddendorf T, Perrett DI. Imitation, mirror neurons and autism. Neurosci Biobehav Rev 2001;25:287–295.
23. Lakin JL, Chartrand TL. Using nonconscious behavioral mimicry to create affiliation and rapport. Psychol Sci 2003;14:334–339.
24. Chartrand TL, Bargh JA. The chameleon effect: the perception-behavior link and social interaction. J Pers Soc Psychol 1999;76: 893–910.
25. Bailenson JN, Yee N. Digital chameleons: automatic assimilation of nonverbal gestures in immersive virtual environments. Psychol Sci 2005;16:814–819.
26. Stewart HJ, McIntosh RD, Williams JHG. A specific deficit of imitation in autism spectrum disorder. Autism Res 2013;6:522–530.
27. Rogers SJ, Hepburn SL, Stackhouse T, Wehner E. Imitation performance in toddlers with autism and those with other developmental disorders. J Child Psychol Psychiatry 2003;44:763–781.
28. McIntosh DN, Reichmann-Decker A, Winkielman P, Wilbarger JL. When the social mirror breaks: deficits in automatic, but not voluntary mimicry of emotional facial expressions in autism. Dev Sci 2006;9:295–302.
29. Oberman LM, Winkielman P, Ramachandran VS. Slow echo: facial EMG evidence for the delay of spontaneous, but not voluntary emotional mimicry in children with autism spectrum disorders. Dev Sci 2009;12:510–520.
30. Dapretto M, Davies MS, Pfeifer JH, et al. Understanding emotions in others: mirror neuron dysfunction in children with autism spectrum disorders. Nat Neurosci 2006;9:28–30.
31. Hadjikhani N, Joseph RM, Snyder J, Tager-Flusberg H. Anatomical differences in the mirror neuron system and social cognition network in autism. Cereb Cortex 2006;16:1276–1282.
32. Biswal B, Mennes M, Zuo XN, et al. Toward discovery science of human brain function. Proc Natl Acad Sci U S A 2010;107:4734–4739.
33. Seeley WW, Menon V, Schatzberg AF, et al. Dissociable intrinsic connectivity networks for salience processing and executive control. J Neurosci 2010;27:2349–2356.
34. Smith S, Fox P, Miller K, et al. Correspondence of the brain's functional architecture during activation and rest. Proc Natl Acad Sci U S A 2009;106:13040–13045.
35. Damoiseaux J, Greicius MD. Greater than the sum of its parts: a review of studies combining structural connectivity and resting-state functional connectivity. Brain Struct Funct 2009;213:525–533.
36. Bullmore E, Sporns O. Complex brain networks: graph theoretical analysis of structural and functional systems. Nat Rev Neurosci 2009;10:186–198.
37. Greicius M, Supekar K, Menon V, Dougherty R. Resting-state functional connectivity reflects structural connectivity in the default mode network. Cereb Cortex 2009;19:72–78.
38. Honey C, Sporns O, Cammoun L, et al. Predicting human resting-state functional connectivity from structural connectivity. Proc Natl Acad Sci U S A 2009;106:2035–2040.
39. Caspers S, Zilles K, Laird AR, Eickhoff SB. ALE meta-analysis of action observation and imitation in the human brain. Neuroimage 2009;50:1148–1167.
40. American Psychiatric Association. Diagnostic and statistical manual of mental disorders, IV-TR. Washington, DC: American Psychiatric Press, 2000.
41. Rutter M, LeCouteur A, Lord C. Autism Diagnostic Interview, Revised (ADI-R). Los Angeles, CA: Western Psychological Services, 2003.
42. Lord C, Rutter M, DiLavore P, Risi S. Autism Diagnostic Observation Schedule. Los Angeles, CA: Western Psychological Services, 2001.
43. Simonoff E, Pickles A, Charman T, et al. Psychiatric disorders in children with autism spectrum disorders: prevalence, comorbidity, and associated factors in a population-derived sample. J Am Acad Child Adolesc Psychiatry 2008;47:921–929.
44. Wechsler D. Wechsler Abbreviated Scale of Intelligence. 2nd ed. San Antonio, TX: Psychological Corporation, 2011.
45. Constantino JN, Gruber CP. Social Responsiveness Scale (SRS) manual. Los Angeles, CA: Western Psychological Services, 2005.
46. Oldfield RC. The assessment and analysis of handedness: the Edinburgh inventory. Neuropsychologia 1971;9:97–113.
47. Cox RW. AFNI: software for analysis and visualization of functional magnetic resonance neuroimages. Comput Biomed Res 1996;29: 162–173.
48. Smith SM, Jenkinson M, Woolrich MW, et al. Advances in functional and structural MR image analysis and implementation as FSL. Neuroimage 2004;23:S208–S219.
49. Cordes D, Haughton VM, Arfanakis K, et al. Frequencies contributing to functional connectivity in the cerebral cortex in "resting-state" data. Am J Neuroradiol 2001;22:1326–1333.
50. Fox MD, Raichle ME. Spontaneous fluctuations in brain activity observed with functional magnetic resonance imaging. Nat Rev Neurosci 2007;8:700–711.

51. Power JD, Barnes KA, Snyder AZ, et al. Spurious but systematic correlations in functional connectivity MRI networks arise from subject motion. Neuroimage 2012;59:2142–2154.

52. Van Dijk KR, Sabuncu MR, Buckner, RL. The influence of head motion on intrinsic functional connectivity MRI. Neuroimage 2012; 59:431–438.

53. Koldewyn K, Yendiki A, Weigelt S, et al. Differences in the right inferior longitudinal fasciculus but no general disruption of white matter tracts in children with autism spectrum disorder. Proc Natl Acad Sci U S A 2014;111:1981–1986.

54. Yendiki A, Koldewyn K, Kakunoori S, et al. Spurious group differences due to head motion in a diffusion MRI study. Neuroimage 2013;88:79–90.

55. Jones DK, Cercignani M. Twenty-five pitfalls in the analysis of diffusion MRI data. NMR Biomed 2010;23:803–820.

56. Wedeen VJ, Wang RP, Schmahmann JD, et al. Diffusion spectrum magnetic resonance imaging (DSI) tractography of crossing fibers. Neuroimage 2008;41:1267–1277.

57. Jbabdi S, Johansen-Berg H. Tractography: where do we go from here? Brain Connect 2011;1:169–183.

58. Schmahmann JD, Pandya DN. Fiber pathways of the brain. New York, NY: Oxford University Press, 2006.

59. Johnson RT, Yeatman JD, Wandell BA, et al. Diffusion properties of major white matter tracts in young, typically developing children. Neuroimage 2014;88:143–154.

60. Johnson MH. Interactive specialization: a domain-general framework for human functional brain development? Dev Cogn Neurosci 2010;1:1–30.

61. Aoki Y, Abe O, Nippashi Y, Yamasue H. Comparison of white matter integrity between autism spectrum disorder subjects and typically developing individuals: a meta-analysis of diffusion tensor imaging tractography studies. Mol Autism 2013;4:25.

62. Syková E, Nicholson C. Diffusion in brain extracellular space. Physiol Rev 2008;88:1277–1340.

63. Peper JS, van den Heuvel MP, Mandl RCW, et al. Sex steroids and connectivity in the human brain: a review of neuroimaging studies. Psychoneuroendocrinology 2011;36:1101–1113.

64. Perrin JS, Herve PY, Leonard G, et al. Growth of white matter in the adolescent brain: role of testosterone and androgen receptor. J Neurosci 2008;28:9519–9524.